Original Article

Cardiac intravoxel incoherent motion diffusion-weighted imaging to assess myocardial microcirculation dysfunction in hypertension

Lei Zhao[1#], Haipeng Wang[2#], Duwang Qiu[1], Liwen Tian[3], Teng Wang[3], Yucheng Yang[2], Yongle Sun[4], Weibo Chen[5], Cuiyan Wang[2]

[1]Department of Radiology, Ji'nan Zhangqiu District People's Hospital, Jinan, China; [2]Department of Radiology, Shandong Provincial Hospital Affiliated to Shandong First Medical University, Jinan, China; [3]Shandong University, Shandong Provincial Hospital, Jinan, China; [4]Department of Cardiology, Shandong Provincial Hospital Affiliated to Shandong First Medical University, Jinan, China; [5]Philips Healthcare, Shanghai, China

Contributions: (I) Conception and design: L Zhao, H Wang, C Wang; (II) Administrative support: C Wang; (III) Provision of study materials or patients: Y Sun; (IV) Collection and assembly of data: D Qiu, L Tian; (V) Data analysis and interpretation: T Wang, Y Yang, W Chen; (VI) Manuscript writing: All authors; (VII) Final approval of manuscript: All authors.

[#]These authors contributed equally to this work.

Correspondence to: Cuiyan Wang, MD, PhD. Department of Radiology, Shandong Provincial Hospital Affiliated to Shandong First Medical University, No. 324 Jingqi Road, Huaiyin District, Jinan 250000, China. Email: wcyzhang@163.com.

Background: Myocardial microcirculation dysfunction is the most potent predictor of adverse cardiovascular events in hypertension. The current study aimed to apply intravoxel incoherent motion diffusion-weighted imaging (IVIM-DWI) to assess hypertension-related microcirculation dysfunction.

Methods: In this prospective study, 102 participants were recruited from our hospital and underwent cardiac magnetic resonance (CMR) examination on a 3T scanning system. Hypertensive patients were divided into 3 subgroups based on blood pressure (BP) types. Two experienced CMR radiologists independently analyzed all images, and Bland-Altman analysis was applied to assess intra- and inter-observer reproducibility. Cardiac function indexes and IVIM-DWI parameters were compared between the hypertension and healthy control groups, as well as among the three hypertension subgroups.

Results: Totally 62 participants with hypertension and 27 healthy controls were included. 13 participants were excluded for poor quality of IVIM-DWI images. Significantly higher maximal left ventricular wall thickness (10.3±2.0 *vs.* 8.6±1.4 mm, P<0.001) and left ventricular mass index (49.0±9.1 *vs.* 42.1±7.5 g/m^2, P<0.05) were observed inhypertension group compared with healthy control group. There were significant statistical differences in pseudo diffusion (D*) between them (81.3±16.3 *vs.* 111.8±18.9 mm^2/s, P<0.001), as well as among the three hypertension subgroups (99.4±13.9 *vs.* 79.7±10.6 *vs.* 67.1±6.6 mm^2/s, P<0.001). Participants with poor quality of IVIM-DWI images had higher heart rates (72.2±10.0 *vs.* 62.0±8.1 bpm, P<0.001).

Conclusions: IVIM-DWI is feasible for quantitatively evaluating myocardial microcirculation dysfunction in hypertension. The D* parameter has a potential value for assessing the severity of microcirculation dysfunction in different BP categories.

Keywords: Hypertension; myocardial microcirculation perfusion; cardiac magnetic resonance (CMR); intravoxel incoherent motion diffusion-weighted imaging (IVIM-DWI); pseudo diffusion (D*)

Submitted Jan 20, 2024. Accepted for publication May 29, 2024. Published online Jul 11, 2024.
doi: 10.21037/qims-24-108
View this article at: https://dx.doi.org/10.21037/qims-24-108

Introduction

Hypertension has been considered the primary and common clinical cardiovascular risk factor for a long time, which often remains undiagnosed or untreated (1,2). Hypertension is closely associated with altered myocardial microcirculation status (3). Myocardial microcirculation, consisting of resistance arteries, arterioles, capillaries, and venules, plays an important role as a common denominator of different heart diseases and has attracted increasing research attention in recent years (4-8). Myocardial microcirculation dysfunction in hypertension mostly manifests by two different types of diffuse structural changes: (I) capillary rarefaction, which consists of abnormally low spatial densities of arterioles, capillaries, and possibly venules, and (II) remodeling of small resistance arteries, which reduces lumen diameter (3,9,10). Myocardial microcirculation dysfunction occurs in the early phases of hypertension (3,10). Persisting hypertension, microcirculation, and microcirculation dysfunction are tightly interconnected into a dangerous cross-link and further worsen cardiac damage (4). Myocardial microcirculation dysfunction is considered the most potent predictor of adverse cardiovascular events in hypertension (3). Quantitative and accurate assessment of myocardial microcirculation dysfunction may provide crucial insights into the pathophysiological processes of hypertension (10,11).

Cardiac magnetic resonance (CMR) is an established noninvasive tool for diagnosing and evaluating cardiac diseases (12,13). Intravoxel incoherent motion diffusion-weighted imaging (IVIM-DWI) is a tool that quantitatively assesses *in vivo* diffusion modeling without contrast agent injection. It has been widely used in various body systems (14-19). Traditional cardiac DWI using ordinary single-index model may reflect myocardial tissue changes at the cellular level and could be applied to assess mean diffusion, including actual water molecule diffusion and random blood flow microcirculation perfusion in the capillary network. Based on non-Gaussian diffusion, IVIM-DWI applies multiple b-value scan imaging to separate actual diffusion and micro-circulation perfusion for the tissue (15-18). IVIM-DWI indexes include the D (reflecting water molecular diffusion), D* (reflecting microcirculation) and f (reflecting perfusion fraction) parameters (20). Due to technical cardiac and respiratory motion restrictions, IVIM-DWI could not apply in CMR until 2003 (21). Recent studies have examined the feasibility and repeatability of IVIM-DWI in characterizing myocardial microcirculation dysfunction in multiple cardiac diseases (22-27). Large sample studies utilizing IVIM-DWI to evaluate myocardial microcirculation dysfunction in hypertension are still required.

This study aimed to assess the value of IVIM-DWI in the assessment of myocardial microcirculation dysfunction in hypertensive patients. We present this article in accordance with the STROBE reporting checklist (available at https://qims.amegroups.com/article/view/10.21037/qims-24-108/rc).

Methods

In this prospective single-center study, 72 hypertensive individuals were recruited from Shandong Provincial Hospital Affiliated to Shandong First Medical University between June 2020 and September 2022 and 30 healthy controls were also enrolled. Inclusion criteria for hypertensive individuals were: (I) 18–65 years old; (II) meeting the diagnostic criteria of hypertension (28) [mean systolic blood pressure (SBP) ≥140 mmHg and/or diastolic blood pressure (DBP) ≥90 mmHg, including individuals with current antihypertensive drug treatment]; (III) no coronary artery diseases, congenital heart diseases, cardiomyopathies, or other medical histories of cardiac diseases; (IV) no systemic diseases that might cause myocardial microcirculation dysfunction, e.g., diabetes, amyloidosis and sarcoidosis; (V) no contraindications for CMR; and (VI) no abnormality on the electrocardiogram (ECG) or detected by echocardiography. Blood pressure (BP) was measured with a clinically validated semiautomatic sphygmomanometer, Omron HEM-737 Intellisense (Omron Healthcare GmbH, Hamburg, Germany). BP measurements were obtained twice after resting for 5 minutes, with ≥2 minutes between measurements before the CMR examination. According to BP categories, patients with hypertension were divided into 3 subgroups, including the H1 (Grade 1 hypertension, 140/90 mmHg ≤ BP ≤159/99 mmHg), H2 (Grade 2 hypertension, 160/100 mmHg ≤ BP ≤179/109 mmHg) and H3 (Grade 3 hypertension, BP ≥180/110 mmHg) groups. The participants meeting the following criteria were included in the healthy control group: (I) mean BP ≤140/90 mmHg; (II) no history of hypertension or anti-hypertensive treatment; (III) no history of cardiac or systemic disease. Baseline demographic and clinical characteristics were recorded. The study was conducted in accordance with the Declaration of Helsinki (as revised in 2013). The study was approved by the ethics committee of Shandong Provincial Hospital Affiliated to Shandong First Medical University (NSFC: No. 2020-382), and written informed consent was obtained from all participants.

CMR imaging protocol

CMR was carried out on a 3.0T clinical MR imaging unit (Philips Healthcare, Amsterdam, Netherlands) with a 16-channel phase-array body coil. The scanning sequences included cine imaging and IVIM-DWI sequences. All cine imaging data were acquired under retrospective electrocardiograph (ECG) trigger and at the end-expiratory condition. Cine images were acquired in the horizontal long axis (HLA) and sequential short axis (SA) orientations from ventricular base to apex. Cine imaging parameters were: repetition time (TR)/echo time (TE), 2.8 ms/1.4 ms; FA, 45°; voxel size, 2.0×2.0×8.0 mm^3. IVIM-DWI was carried out with a tri-directional, single-shot spin-echo echo-planar imaging (EPI) sequence with 8 b values, including 0, 50, 80, 100, 150, 200, 250 and 500 s/mm^2. DWI was conducted along three orthogonal directions simultaneously. Specifically, diffusion gradients were applied along the x, y, and z axes during image acquisition. To compensate for the loss of signal-to-noise ratio (SNR) induced by high b values in IVIM-DWI sequences, different numbers of excitations were applied for different b values: "(0) 1", "(10) 1", "(50) 1", "(100) 2", "(150) 3", "(200) 4", "(250) 5" and "(500) 6". Other imaging parameters were: TR/TE, 1,000/46 ms; matrix size, 160×160; field of view, 310×270 mm^2; slice thickness, 8 mm; Gap, parallel imaging factor sensitivity encoding (SENSE), 3. Cardiac triggering was utilized to minimize motion-related artifacts. A rapid scout axial cine MRI study was carried out to assess the pattern of gross cardiac motion and to identify the optimal imaging window, with the acquisition window placed in the mid-to-late diastolic phase of the cardiac cycle when myocardial motion is minimal. Image acquisition was carried out during free breathing, applying a navigator echo-based respiratory motion compensation technique to further reduce motion artifacts. Motion correction was performed before fitting the IVIM model to ensure the accuracy of the acquired data. Four saturation slabs were set to zero the signal from the areas of chest wall, lung, liver and stomach, immediately above the heart, which may cause artifacts during respiratory motion. Images were acquired in the mid-ventricular SA slice (papillary muscle level). Imaging parameters were: TR, 57 ms; TE, 45.6 ms; matrix size, 96×128; voxel size, 3.0×3.0×8.0 mm^2; acquisition time, 90–180 s.

CMR imaging analysis

All original image data, excluding IVIM-DWI, were analyzed with a commercial postprocessing software, CVI42 (Circle Cardiovascular Imaging Inc., AB, Canada). IVIM-DWI images were post-processed in MITK software (MitkWorkbench, www.mitk.org). Two experienced CMR radiologists (C.W. and H.W., with >5 years of experience in CMR analysis) independently assessed all CMR images. More than 2 weeks later, H.W. repeated the IVIM-DWI image analysis for the assessment of intra-observer agreement. Patients with poor IVIM-DWI image quality (severe artifacts or loss of myocardium signal in >2 IVIM-DWI images with different b values) were excluded from the final analysis.

Left ventricle (LV) cardiac function parameters were assessed in cine images. LV endocardial and epicardial contours were delineated manually for each diastolic and systolic frame in sequential SA cine images. Then, LV cardiac function indexes, including end-diastolic volume (EDV), end-systolic volume (ESV), left ventricle ejection fraction (LVEF) and LV mass, were automatically analyzed. Papillary muscles and trabeculations are part of the ventricular cavity (29). LV cardiac function indexes were standardized by body surface area (BSA) (30). The LV chamber was examined with the American Heart Association (AHA) 17 segments model (apical segments excluded) (31). Maximal LV wall thickness was defined as the most significant linear dimension at any site within the LV myocardium.

IVIM-DWI images were motion-corrected, and a region of interest (ROI) ≥3 mm width was delineated manually on the mid-wall area of the full circumference of the LV in the SA orientation, avoiding the intracardiac blood flow, papillary muscles, and edge pixels (*Figures 1,2*). IVIM-DWI-associated parameters were automatically acquired using a bi-exponential model as follows (32):

$$Sb/S0 = (1-f)\times\exp(-bD) + f\times\exp(-bD^*) \quad [1]$$

The fit method was fit D and f in the higher b-value regime first, then fit D*, as the article of Xiang *et al.* (32). Where S0 is signal intensity at b=0 s/mm^2, Sb is signal intensity at other b values, D reflects tissue structure (water molecular diffusion), D* reflects microcirculation (pseudo diffusion), and f reflects perfusion fraction. The IVIM fitting curves are shown in Figure S1.

Statistical analysis

Statistical Package from the Social Sciences (SPSS, version 26.0, IL, USA) was used for data analysis. Categorical data were presented as percentage (%), and continuous data as mean ± standard deviation (SD) or median (range). The Shapiro-Wilk test was performed to evaluate data normality. Baseline demographic and clinical characteristics were

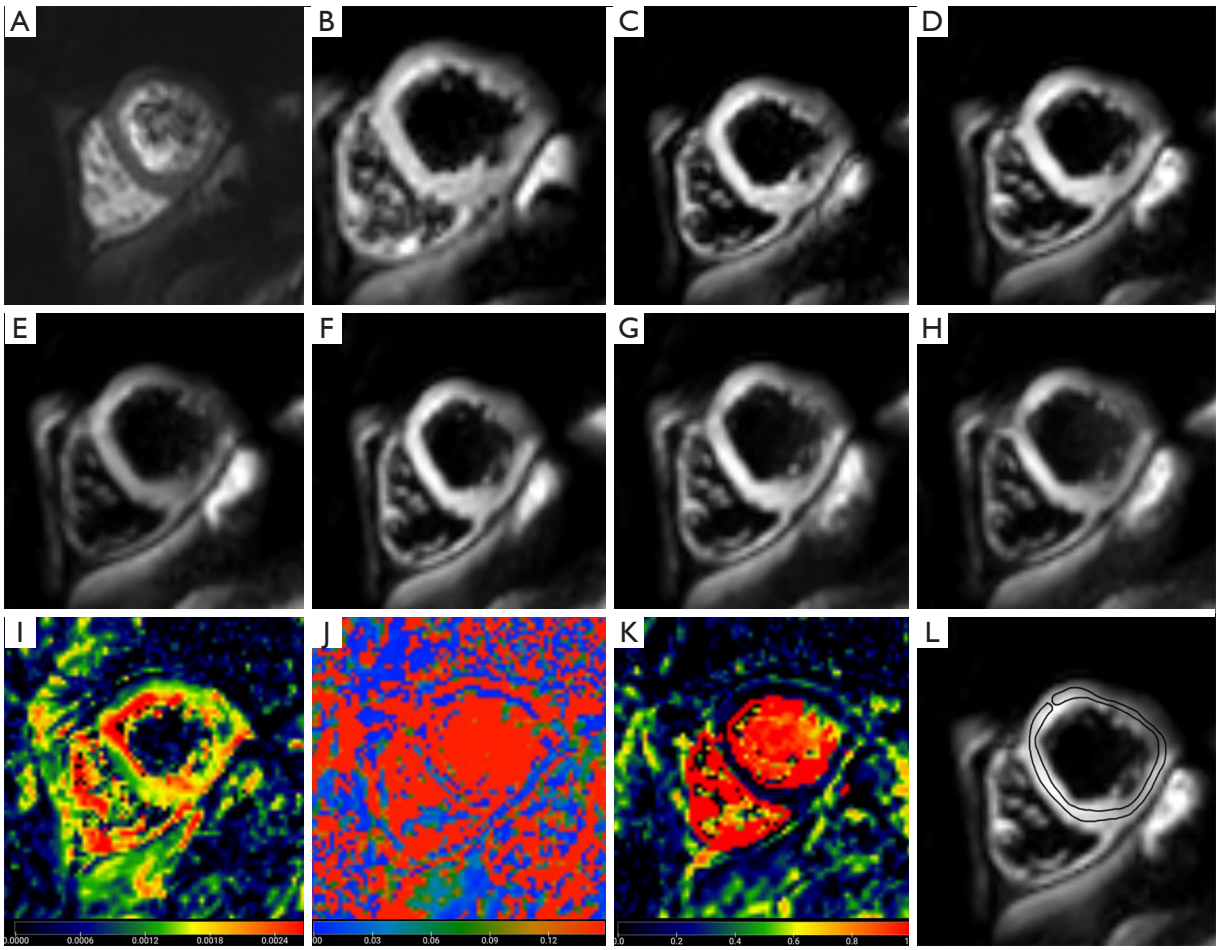

Figure 1 Typical IVIM-DWI images of a 54-year-old male normal subject. (A-H) IVIM-DWI images with different b values (0, 10, 20, 50, 80, 100, 250 and 500 sec/mm^2). The original images were analyzed with the MITK post-processing software, and D (I), D* (J) and f (K) maps were acquired. The ROI region was shown (L). D value: 1.3 mm^2/s; D* value: 120.3 mm^2/s; f value: 12.0%. IVIM-DWI, intravoxel incoherent motion diffusion-weighted imaging; MITK, MitkWorkbench; ROI, region of interest; D, water molecular diffusion; D*, pseudo diffusion; f, perfusion fraction.

compared by the chi-square test for categorical variables, *t*-test and analysis of variance (ANOVA) for normally distributed continuous variables, and the Mann-Whitney U test for skewedly distributed continuous variables. Intra- and Inter-observer reproducibility for various parameters were measured by Bland-Altman analysis and intraclass correlation coefficient (ICC). Two-sided P<0.05 was considered statistically significant.

Results

Clinical characteristics

Totally 62 participants with hypertension (38 males, mean age of 49.9±11.4 years) and 27 healthy controls (12 males, mean age of 49.7±12.5 years) were included in this study. Totally 13 participants were excluded for poor quality of IVIM-DWI images.

In the hypertension group, 17 patients (11 males, mean age of 46.6±14.3 years) were assigned to the H1, 26 (15 males, mean age of 50.5±9.0 years) were assigned to the H2 group, and 19 (12 males, mean age of 53.5±11.9 years) were assigned to the H3 group. There were no significant differences in clinical characteristics between the hypertension and healthy control groups, except for BMI (25.9±2.3 *vs.* 24.5±1.6 kg/m^2, P<0.001). The clinical characteristics of hypertensive patients and healthy controls are presented in *Table 1*.

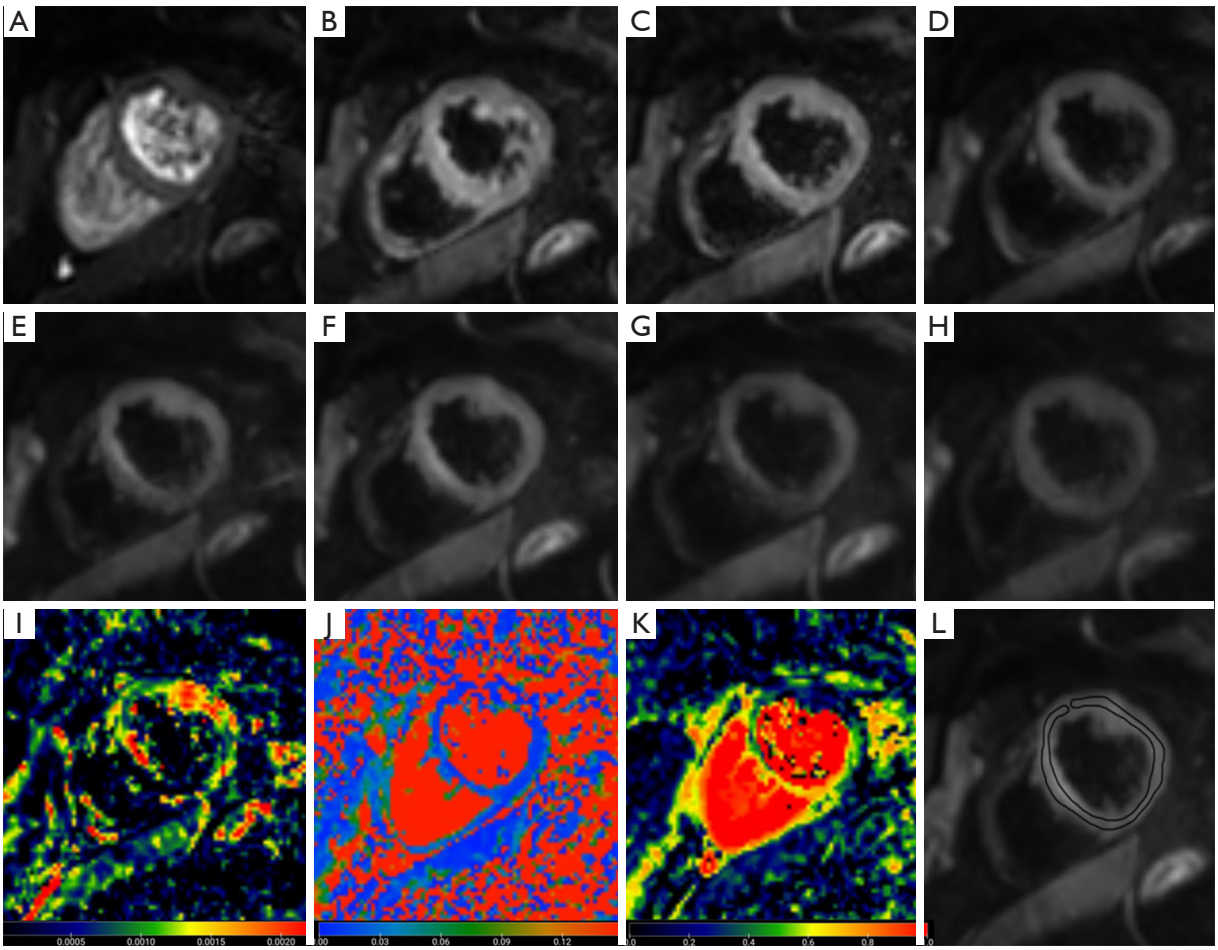

Figure 2 Typical IVIM-DWI images in a 72-year-old female patient with Grade 3 hypertension (very high risk). (A-H) IVIM-DWI images with different b values (0, 10, 20, 50, 80, 100, 250 and 500 sec/mm^2). The original images were analyzed with the MITK post-processing software, and D (I), D* (J) and f (K) maps were acquired. The ROI region was shown (L). D value: 2.0 mm^2/s; D* value: 71.3 mm^2/s; f value: 29.0%. IVIM-DWI, intravoxel incoherent motion diffusion-weighted imaging; MITK, MitkWorkbench; ROI, region of interest; D, water molecular diffusion; D*, pseudo diffusion; f, perfusion fraction.

Table 1 Baseline characteristics of participants

Variable	NC group (N=27)	Hypertension groups (N=62)			P values
		H1 group (N=17)	H2 group (N=26)	H3 group (N=19)	
Sex (M/F)	12/15	11/6	15/11	12/7	0.491
Age (years)	49.7±12.5	46.6±14.3	50.5±9.0	53.5±11.9	0.382
BMI (kg/m^2)	24.5±1.6	24.7±1.7	25.1±1.4	26.9±1.8	<0.001
HR (bpm)	61.1±7.4	63.1±7.7	60.6±8.3	64.2±9.1	0.366
SBP (mmHg)	122.0±7.3	148.3±5.1	168.8±5.5	184.0±5.9	<0.001
DBP (mmHg)	79.5±5.8	94.4±2.9	104.0±4.3	107.4±6.1	<0.001

Data are presented as number or mean ± standard deviation. NC, normal control; H1, Grade 1 hypertension; H2, Grade 2 hypertension; H3, Grade 3 hypertension; M/F, male/female; BMI, body mass index; HR, heart rate; SBP, systolic blood pressure; DBP, diastolic blood pressure.

Table 2 Cardiac function parameters and IVIM-DWI parameters

Parameters	NC group (N=27)	Hypertension groups (N=62)			P values
		H1 group (N=17)	H2 group (N=26)	H3 group (N=19)	
LVEF (%)	59.3±5.2	56.1±5.1	57.1±4.0	56.5±5.6	0.485
LVEDVI (mL/m^2)	73.0±11.7	78.9±11.8	75.3±14.1	73.9±10.2	0.455
LVESVI (mL/m^2)	29.3±5.5	34.3±6.7	32.5±7.6	30.5±6.6	0.076
Max LVWT (mm)	8.6±1.4	10.1±1.3	10.0±1.4	10.8±2.0	<0.001
LV mass index (g/m^2)	42.1±7.5	48.9±7.0	48.5±9.4	49.5±10.9	0.013
D values (mm^2/s)	1.5±0.5	1.6±0.3	1.8±0.5	1.7±0.6	0.221
D* values (mm^2/s)	111.8±18.9	99.4±13.9	79.7±10.6	67.1±6.6	<0.001
F values (%)	22.6±7.0	27.6±11.4	25.6±10.9	26.6±8.7	0.531

Data are presented as mean ± standard deviation. IVIM-DWI, intravoxel incoherent motion diffusion-weighted imaging; NC, normal control; H1, Grade 1 hypertension; H2, Grade 2 hypertension; H3, Grade 3 hypertension; LVEF, left ventricular ejection fraction; LVEDVI, left ventricular end-diastolic volume index; LVESVI, left ventricular end-systolic volume index; Max LVWT, max left ventricular wall thickness; D, water molecular diffusion; D*, pseudo diffusion; F, perfusion fraction.

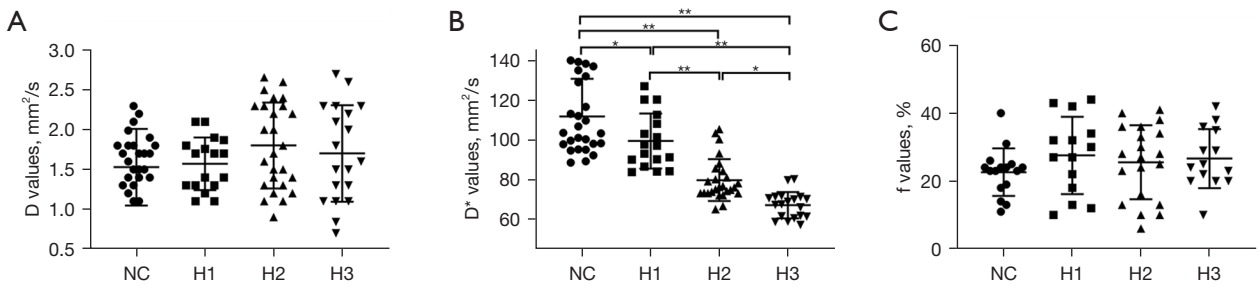

Figure 3 Scatter plots of IVIM-DWI parameters. Scatter plots indicating the distributions of D (A), D* (B) and f (C) values between the hypertension and healthy control groups. Significantly differences in D* values were found between the hypertension and healthy control groups, as well as among the three hypertension subgroups. *, P<0.05; **, P<0.001. NC, normal control; H1, Grade 1 hypertension; H2, Grade 2 hypertension; H3, Grade 3 hypertension; D, water molecular diffusion; D*, pseudo diffusion; f, perfusion fraction; IVIM-DWI, intravoxel incoherent motion diffusion-weighted imaging.

Cardiac function parameters

Standard cardiac function parameters in the hypertension and healthy control groups are shown in *Table 2*. There were significant differences in maximal LV wall thickness (10.3±2.0 *vs.* 8.6±1.4 mm, P<0.001) and LV mass index (49.0±9.1 *vs.* 42.1±7.5 g/m^2, P<0.05) between the hypertension group (including H1–H3 subgroups) and healthy control group, with no statistical differences in other cardiac function parameters.

IVIM-DWI parameters

Compared with the healthy control group, D* values were significantly lower (81.3±16.3 *vs.* 111.8±18.9 mm^2/s, P<0.001) in the hypertension group (including H1–H3 subgroups). There were no significant differences between the two groups in D and f values. Among the three hypertension subgroups, significant differences in D* values were detected (99.4±13.9 *vs.* 79.7±10.6 *vs.* 67.1±6.6 mm^2/s, P<0.001). No significant differences were found in D and f values. The IVIM-DWI images of normal subject are shown in *Figure 1* and the images of a hypertensive patient are shown in *Figure 2*. IVIM-DWI-associated parameters in different groups are shown in *Figure 3* and *Table 2*.

Interobserver and intra-observer variability of IVIM-DWI-associated parameters

Two independent observers analyzed all IVIM-DWI images for assessing inter-observer variability. One observer repeated

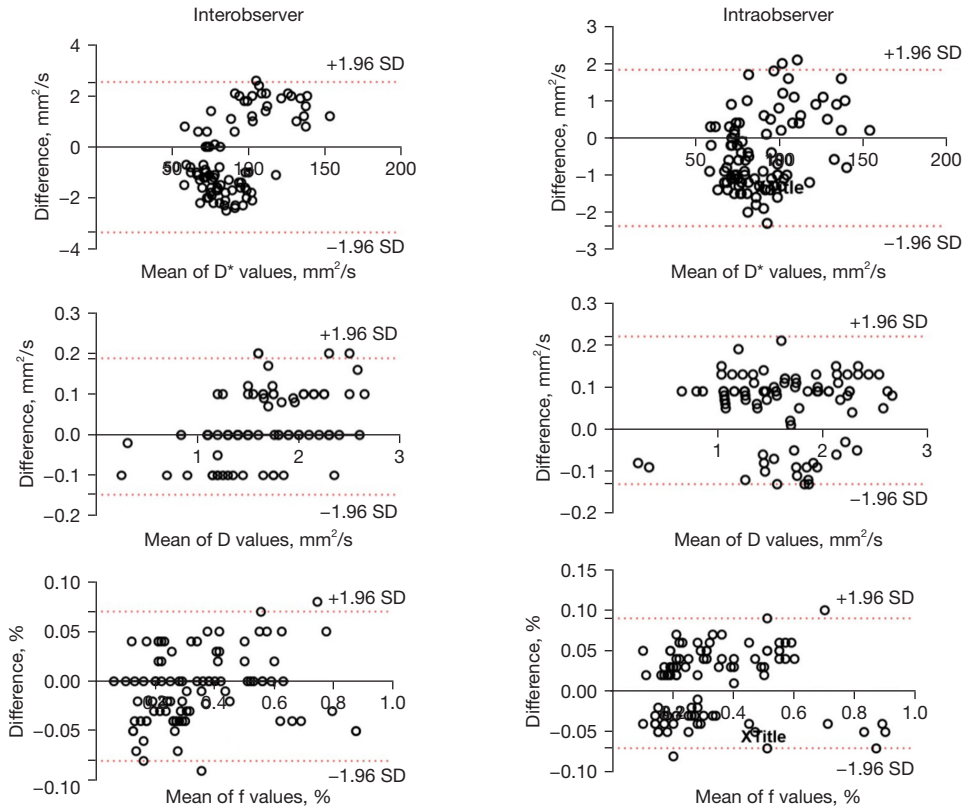

Figure 4 Bland-Altman plots for D, D* and f value measurements indicating good inter-observer and intra-observer agreement. SD, standard deviation; D*, pseudo diffusion; D, water molecular diffusion; f, perfusion fraction.

Table 3 Baseline characteristics of success group and failure group

Variable	Success group (N=89)	Failure group (N=13)	P values
Sex (male)	50 (56.2)	5 (38.5)	0.326
Age (years)	50.2±11.8	52.9±1.6	0.454
BMI (kg/m^2)	25.5±2.5	26.6±2.0	0.149
HR (bpm)	62.0±8.1	72.2±10.0	<0.001
Hypertension	62 (69.7)	8 (61.5)	0.736

Data are presented as n (%) or mean ± standard deviation. BMI, body mass index; HR, heart rate.

the IVIM-DWI image analysis twice within one month for the assessment of intra-observer agreement. Bland-Altman plots for D, D*, and f values are shown in *Figure 4*, indicating good inter-observer and intra-observer agreement.

Factors affecting IVIM-DWI image quality

In this study, 13 participants were excluded because of the poor quality of IVIM-DWI images. Totally 13 participants were included in the failure group and the remaining 89 participants were assigned to the success group. The clinical characteristics were compared between the two groups. A significant difference in heart rate was found between the two groups (62.0±8.1 *vs.* 72.2±10.0 bpm, P<0.001). The clinical characteristics in the failure and success groups are shown in *Table 3*.

Discussion

In this study, the value of IVIM-DWI for the assessment of myocardial microcirculation dysfunction in hypertension was evaluated. We found significant differences in D* values between the hypertension and healthy control groups, as well as among the three hypertension subgroups. IVIM-DWI has proven feasible in the quantitative evaluation of myocardial microcirculation dysfunction in hypertensive patients. D* parameter has a potential value in assessing the severity of microcirculation dysfunction in different BP categories.

Nowadays, the pathophysiology of myocardial microcirculation dysfunction in hypertension has been extensively examined (3-10). Hypertension, myocardial microcirculation, and microcirculation dysfunction are tightly interconnected into a dangerous cross-link (4). Myocardial microcirculation dysfunction can deteriorate cardiac damage resulting from elevated hemodynamic load in hypertension, including LV hypertrophy, impaired systolic and diastolic functions, left atria enlargement, and new onset of atrial fibrillation. The interaction between microcirculation dysfunction, LV hypertrophy, and left ventricular diastolic dysfunction may further promote aortic stiffness, reduce microcirculatory flow reserve, impair tissue perfusion, and induce susceptibility in ischemia (3-5). This study found myocardial microcirculation reflected by IVIM-DWI is impaired in hypertensive individuals, consistent with the pathophysiology of hypertension. The extensively examined pathophysiology of myocardial microcirculation dysfunction in hypertension provided a pathological foundation for this study.

Quantitative and accurate assessment of microcirculation dysfunction is of great significance in providing insights into the pathophysiological features of different cardiovascular diseases. A range of noninvasive and invasive methods are available or emerging for the evaluation of various aspects of microcirculation in animals and humans, each of which has advantages and limitations (33-37). As a "one-stop" exam, CMR could simultaneously assess cardiac anatomy, morphology, function, myocardial perfusion, and myocardial activity (11-13). CMR stress perfusion has been recommended as a routine diagnostic tool to identify inducible myocardial ischemia, and also has a diagnostic and prognostic value in individuals with suspected microcirculation dysfunction (38,39). However, it is hard to apply in clinic. IVIM-DWI is a novel tool to assess myocardial perfusion status. It could quantitatively evaluate *in vivo* diffusion modeling without contrast agent injection. Compared with traditional DWI, IVIM-DWI could provide more details concerning water molecular motion among myocytes, microcirculation, and vascular flow. Recent studies have examined the feasibility and repeatability of IVIM-DWI in characterizing myocardial microcirculation dysfunction in multiple cardiac diseases (22-27). Mou *et al.* performed cardiac IVIM-DWI in patients with hypertrophic cardiomyopathy, diabetes mellitus, and/or hypertension, and found that D* values were significantly lower in patient groups than in healthy volunteers (22). An *et al.* evaluated myocardial perfusion in myocardial infarction patients after percutaneous transluminal coronary intervention (PCI) by IVIM-DWI. The authors demonstrated that D* and f values were significantly reduced at infarct regions (23). Significantly decreased D* and f values were also found in the fibrotic regions of the myocardium in hypertrophic cardiomyopathy patients, indicating impaired myocardial perfusion (25,26). Besides, IVIM-DWI was applied to examine different myocardial perfusion patterns in acute myocardial infarction and infarct-like myocarditis, and lower myocardial perfusion status was detected in acute myocardial infarction (27). The present study found significantly lower D* values in hypertensive patients, corroborating the above report. We found no significant differences in f values between hypertensive patients and healthy controls, which was similar to Mou *et al.* Compared with acute myocardial infarction, infarct-like myocarditis and hypertrophic cardiomyopathy, the myocardium of hypertension shows diffuse and mild myocardial fibrosis. Significant correlations have been determined between IVIM-DWI parameters and myocardial infarct/fibrosis (23-26). There were significantly lower f values at infarct/fibrotic regions of the myocardium, which demonstrated focal and remarkable late gadolinium enhancement (LGE) or increased T1 values/extracellular volume (ECV). The severity of myocardial damage might result from no significant difference in f values. The D* parameter might be utilized as a more sensitive IVIM-DWI index to evaluate myocardial perfusion status compared with the f parameter. We also found significant differences among the three hypertension subgroups in D* values. The negative correlation between D* value and hypertension severity indicated that higher BP could aggravate myocardial microcirculation dysfunction, which was consistent with the pathophysiology of hypertension.

The IVIM-DWI sequence, derived from diffusion-weighted imaging, still remains many deficiencies. First of all, it is very sensitive to the patient's heart and lung motions. Second, the scan time is long because of its multi-b values. Third, the results depend heavily on the fitting methodology (39-41). In this study, respiratory navigator and retrospective ECG gating techniques were applied, and all IVIM-DWI indexes were acquired under free-breathing conditions and end-diastole of the cardiac cycle. Still, 13 participants were excluded from the present analysis because of poor image quality. We analyzed the clinical features of the excluded participants and found significant differences in heart rate between the two groups (62.0±8.1 *vs.* 72.2±10.0 bpm, P<0.001). Our results confirmed heart rate as one of

the essential factors affecting image quality for the IVIM-DWI sequence (22). High heartbeat may shorten the signal acquisition time to decrease image quality. In a further study, heart rate control measurements could be performed to ensure image quality for the IVIM-DWI sequence. In the future, the application of some new technologies, such as diffusion-derived vessel density (DVDD), may reduce these deficiencies and be better applied in clinic (40,41).

This study had several limitations. First, as a novel imaging method to assess myocardial microcirculation status, the diagnostic accuracy of IVIM-DWI has been less examined compared with other methods, including stress perfusion CMR, single photon emission computed tomography and invasive coronary angiography with fractional flow reserve. Furthermore, we recognize the potential benefits of advanced analysis techniques such as tractography or diffusion tensor imaging (DTI), which can provide additional insights into tissue microstructure and connectivity by modeling the diffusion tensor in multiple directions. These techniques may complement ROI-based analyses and offer a more comprehensive understanding of anisotropic diffusion effects. Further studies are required to evaluate its value and potential for further improvement. Secondly, IVIM-DWI images may have artifacts from other bulk flow phenomena, and the number of b values and b value distribution still need further optimization; Suitable software could minimize the misalignment between volumes used averaging of DWIs, such as DIPY (Diffusion Imaging in Python), a library for the analysis of diffusion MRI data (42). It would be of great benefit for our further studies. In addition, motion compensation gradient waveforms in DWI sequences may further improve the quality of DWI images as well as the stability and reliability of IVIM-related parameters. Thirdly, as the hypertension group was subdivided according to BP categories, the sample size of each subgroup was still small.

Conclusions

In conclusion, IVIM-DWI has proven feasible in quantitatively evaluating myocardial microcirculation dysfunction in hypertension. The D* parameter has a potential value in the assessment of the severity of microcirculation dysfunction in different BP categories.

Acknowledgments

Funding: This work was supported by the Shandong Provincial Natural Science Foundation of China Grants (No. ZR2019MH125 to C.W.) and the Shandong Provincial Natural Science Foundation of China Grants (No. ZR2020QH266 to H.W.).

Footnote

Reporting Checklist: The authors have completed the STROBE reporting checklist. Available at https://qims.amegroups.com/article/view/10.21037/qims-24-108/rc

Conflicts of Interest: All authors have completed the ICMJE uniform disclosure form (available at https://qims.amegroups.com/article/view/10.21037/qims-24-108/coif). W.C. reports that he is an MR collaborating scientist from Philips Healthcare providing technical support under the Philips collaboration regulations and has no financial or other conflicts for this study. C.W. reports that study was supported by the Shandong Provincial Natural Science Foundation of China Grants (No. ZR2019MH125). H.W. reports that study was supported by the Shandong Provincial Natural Science Foundation of China Grants (No. ZR2020QH266). The other authors have no conflicts of interest to declare.

Ethical Statement: The authors are accountable for all aspects of the work in ensuring that questions related to the accuracy or integrity of any part of the work are appropriately investigated and resolved. The study was conducted in accordance with the Declaration of Helsinki (as revised in 2013). The study was approved by the ethics committee of Shandong Provincial Hospital Affiliated to Shandong First Medical University (NSFC: No. 2020-382), and written informed consent was obtained from all participants.

References

1. Zhou B, Perel P, Mensah GA, Ezzati M. Global

epidemiology, health burden and effective interventions for elevated blood pressure and hypertension. Nat Rev Cardiol 2021;18:785-802.
2. Benas D, Triantafyllidi H, Birmpa D, Fambri A, Schoinas A, Thymis I, Kostelli G, Ikonomidis I. Hypertension-Mediated Organ Damage In Young Patients With First-Diagnosed And Never Treated Systolic Hypertension. Curr Vasc Pharmacol 2023;21:197-204.
3. Zdravkovic M, Popadic V, Klasnja S, Klasnja A, Ivankovic T, Lasica R, Lovic D, Gostiljac D, Vasiljevic Z. Coronary Microvascular Dysfunction and Hypertension: A Bond More Important than We Think. Medicina (Kaunas) 2023;59:2149.
4. Laurent S, Agabiti-Rosei C, Bruno RM, Rizzoni D. Microcirculation and Macrocirculation in Hypertension: A Dangerous Cross-Link? Hypertension 2022;79:479-90.
5. Gutterman DD, Chabowski DS, Kadlec AO, Durand MJ, Freed JK, Ait-Aissa K, Beyer AM. The Human Microcirculation: Regulation of Flow and Beyond. Circ Res 2016;118:157-72.
6. Dong F, Yin L, Sisakian H, Hakobyan T, Jeong LS, Joshi H, et al. Takotsubo syndrome is a coronary microvascular disease: experimental evidence. Eur Heart J 2023;44:2244-53.
7. Gao J, Meng T, Li M, Du R, Ding J, Li A, Yu S, Li Y, He Q. Global trends and frontiers in research on coronary microvascular dysfunction: a bibliometric analysis from 2002 to 2022. Eur J Med Res 2022;27:233.
8. Bradley C, Berry C. Definition and epidemiology of coronary microvascular disease. J Nucl Cardiol 2022;29:1763-75.
9. De Ciuceis C, Rizzoni D, Palatini P. Microcirculation and Physical Exercise In Hypertension. Hypertension 2023;80:730-9.
10. Yang Z, Liu Y, Li Z, Feng S, Lin S, Ge Z, Fan Y, Wang Y, Wang X, Mao J. Coronary microvascular dysfunction and cardiovascular disease: Pathogenesis, associations and treatment strategies. Biomed Pharmacother 2023;164:115011.
11. Roman MJ, Devereux RB. Association of central and peripheral blood pressures with intermediate cardiovascular phenotypes. Hypertension 2014;63:1148-53.
12. Di Marco A. Cardiac Magnetic Resonance and Ventricular Arrhythmias: An Indissoluble Liaison. JACC Cardiovasc Imaging 2023;16:1550-1.
13. Francone M, Figliozzi S, Monti L, Loewe C, Catapano F. Multiparametric cardiac magnetic resonance unveiling the mechanisms and early manifestations of anticancer drug cardiotoxicity. Eur Radiol 2023;33:8439-41.
14. Mesny E, Leporq B, Chapet O, Beuf O. Intravoxel incoherent motion magnetic resonance imaging to assess early tumor response to radiation therapy: Review and future directions. Magn Reson Imaging 2024;108:129-37.
15. Pavilla A, Gambarota G, Signaté A, Arrigo A, Saint-Jalmes H, Mejdoubi M. Intravoxel incoherent motion and diffusion kurtosis imaging at 3T MRI: Application to ischemic stroke. Magn Reson Imaging 2023;99:73-80.
16. Zhou B, Zhou Y, Tang Y, Bao Y, Zou L, Yao Z, Feng X. Intravoxel incoherent motion MRI for rectal cancer: correlation of diffusion and perfusion characteristics with clinical-pathologic factors. Acta Radiol 2023;64:898-906.
17. Sheng Y, Dang X, Zhang H, Rui W, Wang J, Cheng H, Qiu T, Zhang Y, Ding Y, Yao Z, Pang H, Ren Y. Correlations between intravoxel incoherent motion-derived fast diffusion and perfusion fraction parameters and VEGF- and MIB-1-positive rates in brain gliomas: an intraoperative MR-navigated, biopsy-based histopathologic study. Eur Radiol 2023;33:5236-46.
18. Yin P, Xu J, Sun X, Liu T, Chen L, Hong N. Intravoxel incoherent motion and dynamic contrast-enhanced magnetic resonance imaging for neoadjuvant chemotherapy response evaluation in patients with osteosarcoma. Eur J Radiol 2023;162:110790.
19. Bartsch SJ, Brožová K, Ehret V, Friske J, Fürböck C, Kenner L, Laimer-Gruber D, Helbich TH, Pinker K. Non-Contrast-Enhanced Multiparametric MRI of the Hypoxic Tumor Microenvironment Allows Molecular Subtyping of Breast Cancer: A Pilot Study. Cancers (Basel) 2024;16:375.
20. Le Bihan D, Breton E, Lallemand D, Aubin ML, Vignaud J, Laval-Jeantet M. Separation of diffusion and perfusion in intravoxel incoherent motion MR imaging. Radiology 1988;168:497-505.
21. Callot V, Bennett E, Decking UK, Balaban RS, Wen H. In vivo study of microcirculation in canine myocardium using the IVIM method. Magn Reson Med 2003;50:531-40.
22. Mou A, Zhang C, Li M, Jin F, Song Q, Liu A, Li Z. Evaluation of myocardial microcirculation using intravoxel incoherent motion imaging. J Magn Reson Imaging 2017;46:1818-28.
23. An DA, Chen BH, Rui-Wu, Shi RY, Bu J, Ge H, Hu J, Xu JR, Wu LM. Diagnostic performance of intravoxel incoherent motion diffusion-weighted imaging in the assessment of the dynamic status of myocardial perfusion.

J Magn Reson Imaging 2018;48:1602-9.
24. Terrier B, Dechartres A, Gouya H, Ben Arfi M, Bérézne A, Régent A, Dunogué B, London J, Cohen P, Guillevin L, Le Jeunne C, Legmann P, Vignaux O, Mouthon L. Cardiac Intravoxel Incoherent Motion Diffusion-Weighted Magnetic Resonance Imaging With T1 Mapping to Assess Myocardial Perfusion and Fibrosis in Systemic Sclerosis: Association With Cardiac Events From a Prospective Cohort Study. Arthritis Rheumatol 2020;72:1571-80.
25. Xiang X, Lin X, Zhang B, Lin C, Lei J, Guo S, Zhao S. Microvascular Dysfunction Associates With Outcomes in Hypertrophic Cardiomyopathy: Insights From the Intravoxel Incoherent Motion MRI. J Magn Reson Imaging 2023;57:1766-75.
26. Wu R, An DA, Shi RY, Chen BH, Wu CW, Jiang M, Xu JR, Wu LM, Pu J. The feasibility and diagnostic value of intravoxel incoherent motion diffusion-weighted imaging in the assessment of myocardial fibrosis in hypertrophic cardiomyopathy patients. Eur J Radiol 2020;132:109333.
27. An DA, Shi RY, Wu R, Suo S, Han TT, Xu JR, Pu J, Wu LM. Different Myocardial Perfusion Status in Acute Myocardial Infarction and Infarct-like Myocarditis: A Novel Intravoxel Incoherent Motion Diffusion-weighted Imaging based MRI Study. Acad Radiol 2020;27:1093-102.
28. Writing Group of 2018 Chinese Guidelines for the Management of Hypertension, Chinese Hypertension League, Chinese Society of Cardiology, Chinese Medical Doctor Association Hypertension Committee, Hypertension Branch of China International Exchange and Promotive Association for Medical and Health Care, Hypertension Branch of Chinese Geriatric Medical Association. 2018 Chinese guidelines for the management of hypertension. Chin J Cardiovasc Med 2019;24:24-56.
29. Buechel EV, Kaiser T, Jackson C, Schmitz A, Kellenberger CJ. Normal right- and left ventricular volumes and myocardial mass in children measured by steady state free precession cardiovascular magnetic resonance. J Cardiovasc Magn Reson 2009;11:19.
30. Kawel-Boehm N, Maceira A, Valsangiacomo-Buechel ER, Vogel-Claussen J, Turkbey EB, Williams R, Plein S, Tee M, Eng J, Bluemke DA. Normal values for cardiovascular magnetic resonance in adults and children. J Cardiovasc Magn Reson 2015;17:29.
31. Cerqueira MD, Weissman NJ, Dilsizian V, Jacobs AK, Kaul S, Laskey WK, Pennell DJ, Rumberger JA, Ryan T, Verani MS; American Heart Association Writing Group on Myocardial Segmentation and Registration for Cardiac Imaging. Standardized myocardial segmentation and nomenclature for tomographic imaging of the heart. A statement for healthcare professionals from the Cardiac Imaging Committee of the Council on Clinical Cardiology of the American Heart Association. Circulation 2002;105:539-42.
32. Xiang SF, Zhang XQ, Yang SJ, Gao YY, Gao BL, Shi QL, Li S. Intravoxel Incoherent Motion Magnetic Resonance Imaging with Integrated Slice-specific Shimming for old myocardial infarction: A Pilot Study. Sci Rep 2019;9:19766.
33. Wang D, Li X, Feng W, Zhou H, Peng W, Wang X. Diagnostic and prognostic value of angiography-derived index of microvascular resistance: a systematic review and meta-analysis. Front Cardiovasc Med 2024;11:1360648.
34. Schindler TH, Fearon WF, Pelletier-Galarneau M, Ambrosio G, Sechtem U, Ruddy TD, et al. Myocardial Perfusion PET for the Detection and Reporting of Coronary Microvascular Dysfunction: A JACC: Cardiovascular Imaging Expert Panel Statement. JACC Cardiovasc Imaging 2023;16:536-48.
35. Rigattieri S, Barbato E, Berry C. Microvascular resistance reserve: a reference test of the coronary microcirculation? Eur Heart J 2023;44:2870-2.
36. Madias JE. Towards refining of the proposed ECG-based index of coronary microvascular resistance (ECGMVR). J Electrocardiol 2023;80:111-8.
37. Hendel RC, Friedrich MG, Schulz-Menger J, Zemmrich C, Bengel F, Berman DS, Camici PG, Flamm SD, Le Guludec D, Kim R, Lombardi M, Mahmarian J, Sechtem U, Nagel E. CMR First-Pass Perfusion for Suspected Inducible Myocardial Ischemia. JACC Cardiovasc Imaging 2016;9:1338-48.
38. Coelho-Filho OR, Jerosch-Herold M. Stress-Only CMR Perfusion: Ready for Clinical Application? Circ Cardiovasc Imaging 2023;16:e016147.
39. Yarahmadi P, Forouzannia SM, Forouzannia SA, Malik SB, Yousefifard M, Nguyen PK. Prognostic Value of Qualitative and Quantitative Stress CMR in Patients With Known or Suspected CAD. JACC Cardiovasc Imaging 2024;17:248-65.
40. Li XM, Yao DQ, Quan XY, Li M, Chen W, Wáng YXJ. Perfusion of hepatocellular carcinomas measured by diffusion-derived vessel density biomarker: Higher hepatocellular carcinoma perfusion than earlier intravoxel incoherent motion reports. NMR Biomed

2024;37:e5125.
41. Yu WL, Xiao BH, Ma FZ, Zheng CJ, Tang SN, Wáng YXJ. Underestimation of the spleen perfusion fraction by intravoxel incoherent motion MRI. NMR Biomed 2023;36:e4987.
42. Garyfallidis E, Brett M, Amirbekian B, Rokem A, van der Walt S, Descoteaux M, Nimmo-Smith I; Dipy Contributors. Dipy, a library for the analysis of diffusion MRI data. Front Neuroinform 2014;8:8.

Cite this article as: Zhao L, Wang H, Qiu D, Tian L, Wang T, Yang Y, Sun Y, Chen W, Wang C. Cardiac intravoxel incoherent motion diffusion-weighted imaging to assess myocardial microcirculation dysfunction in hypertension. Quant Imaging Med Surg 2024;14(8):5346-5357. doi: 10.21037/qims-24-108

